

Phase transitions in single macromolecules: Loop-stretch transition versus loop adsorption transition in end-grafted polymer chains

Shuangshuang Zhang,^{1,2,3} Shuanhu Qi,^{4,*} Leonid I. Klushin,^{5,6}
Alexander M. Skvortsov,⁷ Dadong Yan,¹ and Friederike Schmid⁴

¹*Department of Physics, Beijing Normal University, Beijing 100875, China*

²*Department of Basic Courses, Tianjin Sino-German University of Applied Sciences, Tianjin 300350, China*

³*Graduate School Of Excellence Materials Science in Mainz, Staudingerweg 9, D-55128 Mainz, Germany*

⁴*Institut für Physik, Johannes Gutenberg-Universität Mainz, Staudingerweg 9, D-55099 Mainz, Germany*

⁵*Department of Physics, American University of Beirut, P. O. Box 11-0236, Beirut 1107 2020, Lebanon*

⁶*Institute for Macromolecular Compounds RAS, Bolshoi pr. 31, 199004 St.Petersburg, Russia*

⁷*Chemical-Pharmaceutical Academy, Professora Popova 14, 197022 St. Petersburg, Russia*

We use Brownian dynamics simulations and analytical theory to compare two prominent types of single molecule transitions. One is the adsorption transition of a loop (a chain with two ends bound to an attractive substrate) driven by an attraction parameter ε , and the other is the loop-stretch transition in a chain with one end attached to a repulsive substrate, driven by an external end-force F applied to the free end. Specifically, we compare the behavior of the respective order parameters of the transitions, i.e., the mean number of surface contacts in the case of the adsorption transition, and the mean position of the chain end in the case of the loop-stretch transition. Close to the transition points, both the static and the dynamic behavior of chains with different length N are very well described by a scaling Ansatz with the scaling parameters $(\varepsilon - \varepsilon^*)N^\phi$ (adsorption transition) and $(F - F^*)N^\nu$ (loop-stretch transition), respectively, where ϕ is the crossover exponent of the adsorption transition, and ν the Flory exponent. We show that both the loop-stretch and the loop adsorption transitions provide an exceptional opportunity to construct explicit analytical expressions for the crossover functions which perfectly describe all simulation results on static properties in the finite-size scaling regime. Explicit crossover functions are based on the Ansatz for the analytical form of the order parameter distributions at the respective transition points. In contrast to the close similarity in equilibrium static behavior, the dynamic relaxation at the two transitions shows qualitative differences, especially in the strongly ordered regimes. This is attributed to the fact that the surface contact dynamics in a strongly adsorbed chain is governed by local processes, whereas the end height relaxation of a strongly stretched chain involves the full spectrum of Rouse modes.

I. INTRODUCTION

Grafted polymers have attracted great attention in the past few decades due to their potential applications in surface modification, functional surface manufacturing, or sensors [1–6]. At the level of single molecules, chain adsorption and chain stretching are among the most prominent fundamental processes [7]. For example, the adsorption of polymers at interfaces can significantly modify interfacial properties such as the friction coefficient [8]. On the other hand, tension-induced stretching is used in modern micromanipulation experiments to characterize the elastic properties of biological molecules such as DNA or proteins [9–11]. Thus, studying the physics of these two processes is of basic interest.

In previous work [12, 13], two of us have pointed out a fundamental analogy between the adsorption transition and the loop-stretch transition of single end-grafted ideal chains. The adsorption transition in the absence of external force ($F = 0$) has been studied intensively for many decades [14, 15]. It is driven by the competition between the effective repulsion imposed by a hard substrate, and an additional attractive interaction with

monomers. The effective repulsion is due to the loss of configurational entropy associated with each contact of the chain with the impenetrable substrate. If the attractive interaction is weaker than the entropic repulsion, the tethered chain avoids touching neutral surfaces and assumes a coiled “mushroom” configuration. As soon as the attractive energy exceeds a certain value ε^* and overcomes the entropic loss, the chain starts adsorbing onto the substrate. For chains of infinite length, $\varepsilon = \varepsilon^*$ turns out to be a critical point. The fraction of monomers in contact with the substrate plays the role of the order parameter conjugated to the control parameter ε .

The loop-stretch transition can be observed when a constant force is applied to the free chain end along the normal direction while the other end is grafted to the substrate. Now, the system is characterized by yet another order parameter conjugated to the end force, F : it has the meaning of the chain stretching and is given by the free end height, Z divided by the chain contour length [13, 16–19]. On strongly attractive surfaces the stretching force drives a sharp transition known as mechanical desorption which turns out to be first order in the infinite chain length limit. Whereas this transition has been studied quite extensively [20–23], the situation when the grafting surface is weakly attractive or purely repulsive has received much less attention. Here, one can

* qish@uni-mainz.de

still identify a force-driven transition in the infinite chain limit [16] (Fig. 1, left arrow). Depending on the sign of the normal force there appears two types of chain conformations. Namely, the stretching order parameter tends to zero when the chain end is pressed onto the substrate (negative force pointing towards the substrate), or to a finite non-zero limit when the force points away from the substrate.

At infinite chain length $N \rightarrow \infty$, the interplay of the loop-stretch transition and the adsorption transitions leads to a phase diagram in the $F - \varepsilon$ plane which is schematically sketched in Fig. 1 [13]: Two lines of second order transition, corresponding to loop-stretch transitions and adsorption transitions, meet at a bicritical point, which is also the end point of a line of first order transitions between the zipped and unzipped state on strongly attractive surfaces. Since a standard discussion of the adsorption transition does not include any end force, this bicritical point is implicitly identified with the regular critical adsorption point.

For an ideal continuum Gaussian chain in the presence of a normal end force and a surface pseudopotential (which could change from attraction to repulsion) one can establish a formally exact symmetry between the effects of the force and the surface potential [12, 13]. It follows from this symmetry that for a given chain length, N , the functional dependence of the average height of the free end, $\langle Z \rangle$, on the external force, F , in the loop-stretch transition (at $\varepsilon = 0$) is the same as the dependence of the average number of adsorbed segments, $\langle m \rangle$, on the adsorption strength, ε , in the adsorption transition (at $F = 0$). In the infinite chain limit, it is known that the free energy for the adsorption of a loop is identical to that of a chain [24]. In both transitions, finite-size effects are described by ideal crossover indices (both equal to $1/2$) and the same crossover function. The critical behavior at both transitions can be evaluated within a Landau expansion and is characterized by mean field critical exponents [12].

Real chains in good solvent are swollen and the critical behavior in the above transitions changes. The exponent characterizing the extension of a chain as a function of chain length N changes from $\nu = 1/2$ for random walk to the Flory exponent $\nu = 0.588$ for self-avoiding walks [14, 25]. In the vicinity of the adsorption transition, an independent crossover exponent ϕ [15] comes into play, which characterizes the scaling of the number of contacts with N right at the critical point. This exponent is not relevant for the loop-stretch transition. Therefore, one no longer has an exact quantitative correspondence. At a qualitative level, however, one still expects the loop adsorption transition and the loop-stretch transition of real grafted chains to share similar thermodynamic features.

The situation is different when looking at dynamics. Critical singularities in thermodynamic fluctuations are typically associated with critical slowing down, and this is also expected here. Beyond that, however, the kinetic behavior of the two microscopic observables Z and m

with respect to F and ε should be considerably different. The observable Z characterizing the loop-stretch transition fluctuates as a result of cooperative motion of monomers involving a full spectrum of Rouse modes whereas the observable m characterizing the adsorption-desorption transition fluctuates due to weakly correlated formation and destruction of monomer contacts separated by large contour length distances. Thus one expects qualitative differences in the dynamic behavior at the two transitions.

The purpose of the present paper is to present a systematic comparison of the loop-stretch transition and the desorption-adsorption transition, both with respect to static and dynamic behavior. We employ Brownian dynamics (BD) simulations to investigate the thermodynamic and kinetic behavior of a single polymer chain grafted onto an impenetrable substrate in the vicinity of the transitions. To avoid multicritical crossover phenomena, the specific transition points in the $F - \varepsilon$ plane are chosen such that they are far from the bicritical point (see Fig. 1). Hence, we study the loop-stretch transition at $\varepsilon = 0$ and the desorption-adsorption transition at strongly negative F , i.e the adsorption of a loop. The simulations are complemented by theoretical considerations. Our results confirm and quantify the similarity in the thermodynamic behavior at the two transitions, and demonstrate the differences in the relaxation dynamics.

The paper is organized in the following way. In Sec. II the model system and BD scheme are briefly described. Section III presents the analytical theory as well as dynamic simulation results for the loop-stretch and adsorption transitions. Both static and dynamic properties are discussed in detail. Section IV summarizes the present work. Finally, an Appendix gives some detailed formulations about the BD scheme.

II. MODEL AND METHODS

We consider a polymer chain of N beads connected by Gaussian elastic springs inside an $L \times L \times H$ box. Throughout this paper, we express all lengths in unit of the statistical segment length a , energies in unit of $k_B T$, and times in unit of $\zeta_0 a^2$, where ζ_0 is the friction coefficient for each bead. We further use $L = 4\sqrt{N}$ and $H = N$, and implement periodic boundary conditions in the x and y directions and impenetrable boundaries in z direction. One end of the chain is anchored on the impenetrable surface at $z = 0$. To model the stretching process, an external force F , the direction of which is normal to the surface, is applied to the free end of the chain. To model the adsorption process, an additional short-range monomer-surface interaction is introduced *via* a surface potential $-\varepsilon U_a(\mathbf{r})$ with $U_a(\mathbf{r}) = \min(1, 3/2 - z)$ (for $z < 3/2$). The strength of adsorption ε corresponds to the energy gain if a monomer is in contact with the substrate. The non-bonded interactions between segments are described by a coarse grained soft potential, which

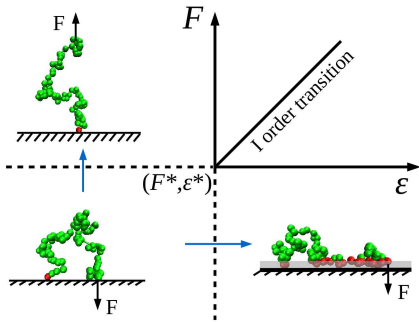


FIG. 1. Schematic sketch of phase diagram for chains of infinite length in the plane of external end force F and adsorption parameter ε , showing the two transitions investigated in the present work: The loop-stretch transition (left blue arrow, pointing upwards), and the adsorption transition (right blue arrow, pointing to the right). The transition points are chosen such that they are far from the bicritical point at (F^*, ε^*) . Therefore, the adsorption transition is studied in the presence of a negative end force. The order parameter characterizing the loop-end transition is the distance of the chain end from the surface. The order parameter of the desorption-adsorption transition is the number of chain contacts with the surface (number of red dots).

depends on the local number density of segments and is evaluated on a grid in the spirit of the Particle-to-Mesh approach [26–28] with grid size $b = 1$. The parameter b can be interpreted as a coarse-graining length. The total Hamiltonian is then given by

$$\mathcal{H}_s = \frac{3}{2} \sum_{j=2}^N (\mathbf{R}_j - \mathbf{R}_{j-1})^2 + \frac{v}{2} \sum_{\alpha} \hat{\rho}_{\alpha}^2 \quad (1)$$

$$- F Z_1 - \varepsilon \sum_{j=1}^{N-1} U_{\alpha}(Z_j)$$

where \mathbf{R}_j denotes the location of the j th bead, Z_j the corresponding z -component (with $Z_N = 0$), α runs over all grid points, and $\hat{\rho}_{\alpha}$ denotes the local density at the grid point α . Specifically, $\hat{\rho}_{\alpha}$ is determined from the particle positions \mathbf{R}_j using the Cloud-in-Cells (CIC) assignment scheme [29], with cloud/cell size b and the z -components of the vertices located at $z = 0.5 + n$ ($n \in \mathbb{N}_0$). To simplify the notation for the coordinate of the free end which is one of the main quantities of interest, in the rest of the paper we drop the subscript: $Z_1 \equiv Z$.

The excluded volume parameter v is set to $v = 1$ such that the grafted polymer is in a good (implicit) solvent. The bead positions evolve according to the equations of over-damped Brownian dynamics, i.e.,

$$\dot{\mathbf{R}}_j = -\partial\mathcal{H}/\partial\mathbf{R}_j + \sqrt{2}\mathbf{f}_r \quad (2)$$

where \mathbf{f}_r is an uncorrelated Gaussian random force with mean zero and variance $\langle f_{r\alpha}(t)f_{r\beta}(t') \rangle = \delta_{\alpha\beta}\delta(t-t')$ ($\alpha, \beta = x, y, z$). The time step for integrating the dynamics equations is chosen as $\Delta t = 0.005$. For details of the BD simulation scheme, we refer to the Appendix.

The Hamiltonian (1) is used to simulate the stretching process by setting $\varepsilon = 0$ and varying F , and to simulate the adsorption process by setting $F = -2$ and varying ε . Statistics are performed for the order parameters of the two processes, i.e., Z for the chain stretching case and the number of adsorbed segments m for the chain adsorption case. Here, m is defined as the number of segments that experience the surface adsorption potential, i.e., the number of segments with a distance less than $d = 1$ from the surface. The stretching degree ξ and the fraction of adsorbed segments θ are defined as Z/N and m/N , respectively.

III. RESULTS AND DISCUSSION

A. Characterization of the phase transitions

We begin with characterizing the thermodynamic properties by examining the behavior of order parameters and fluctuations. The degree of stretching $\xi = Z/N$ serves as the order parameter in the loop-stretch problem, where Z is the distance between the free end and the substrate. Accordingly, the order parameter in the problem of chain adsorption is the fraction of adsorbed segments $\theta = m/N$, where m is the number of adsorbed segments.

The adsorption of a single chain with excluded volume effects (in the force free case $F = 0$) has a long history of exploration. Monte Carlo (MC) and MD simulations were used for both lattice and off-lattice models. Two difficult problems have to be tackled: The accurate determination of the critical point, where several methods were proposed and tested, and the evaluation of the near-critical behavior in the framework of the crossover scaling hypothesis. By comparison, the loop-stretch transition happens to be much more straightforward; this may be a reason why it was never studied in detail by simulations. On the other hand, we will show below that it has the advantage of admitting an analytical solution.

Figs. 2(a) and (b) show the ensemble averages $\langle \xi \rangle$ and $\langle \theta \rangle$ as a function of the applied force F and the adsorption strength ε , respectively. In both cases, the order parameter is a continuous function of the control variable, with an initial slowly increasing part followed by a rapidly increasing region. As the chain length increases, it can be seen that the crossover between these two regions narrows. Albeit hard to achieve numerically, it can be expected that in the infinite chain limit $N \rightarrow \infty$, the slope becomes discontinuous at a threshold point indicating a continuous phase transition in both cases [18].

The critical force value $F^* = 0$ for the loop-stretch transition can be conjectured intuitively. In the infinite chain limit $N \rightarrow \infty$ at $F = 0$ the average stretching order parameter of the mushroom conformation $\langle Z \rangle/N \sim N^{\nu-1}$ tends to zero. The surface potential is short-ranged and has no direct relevance as long as it is non-adsorbing. In the same limit the elasticity of the mushroom van-

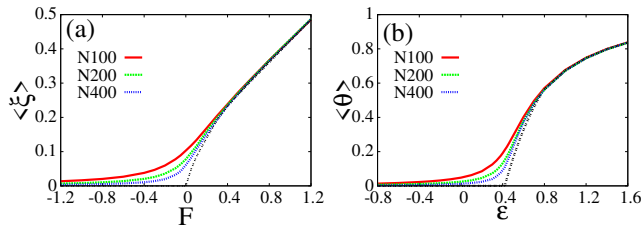


FIG. 2. (a) Average stretching degree $\langle \xi \rangle$ as a function of stretching force F for the loop-stretch transition at $\varepsilon = 0$ and (b) average fraction of adsorbed segments $\langle \theta \rangle$ as a function of adsorption strength ε for the adsorption transition at $F = -2$ for three chain lengths $N = 100, 200, 400$ as indicated. Black dashed lines show the extrapolation to the infinite chain limit $N \rightarrow \infty$.

ishes. Hence an arbitrary small (but N -independent) positive end force would produce a nonzero strain. We conclude that the mushroom state at $F = 0$ is, indeed a critical state. A more formal rigorous way to locate critical points from the numerical data is the Binder cumulant method [30]. We use the 2nd order cumulants and determine the critical point as the intersection point of the curves for $\sigma^2(O)/\langle O \rangle^2$ for different chain lengths N , where O is the relevant order parameter ($O = Z$ and $O = m$, respectively) and the variance $\sigma^2(O) = \langle O^2 \rangle - \langle O \rangle^2$ quantifies its fluctuations. The corresponding numerical results, displayed in Fig. 3, give $\varepsilon^* = 0.42 \pm 0.01$ and $F^* = 0$. We notice that the latter result is consistent with the recent studies of self-avoiding walks under stretching [20, 21].

Next we study the behavior of the order parameter and the fluctuations σ^2 as a function of the control parameter, i.e., the conjugate parameter that drives the transition – the force F in the case of the loop-stretch transition, and the adsorption strength ε in the case of the adsorption transition. The results are shown and compared to each other in Fig. 4. Parts (a) and (c) refer to the loop-stretch transition (at $\varepsilon = 0$) and show the chain end position $\langle Z \rangle$ and $\sigma^2(Z)$, respectively, as a function of the stretching force F . Parts (c) and (d) refer to the adsorption transition (at $F = -2$) and show the number of contacts m and $\sigma^2(m)$ as a function of the adsorp-

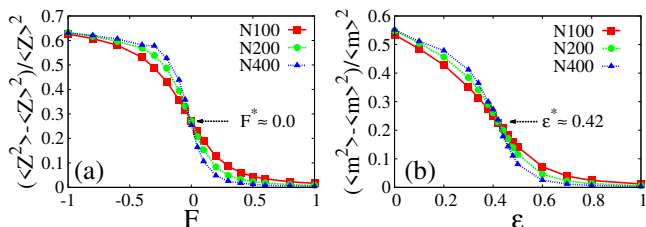


FIG. 3. Second order Binder cumulants (a) for the loop-stretch transition at $\varepsilon = 0$, (b) for the adsorption transition at $F = -2$. The curves for different chain lengths N intersect at the critical point.

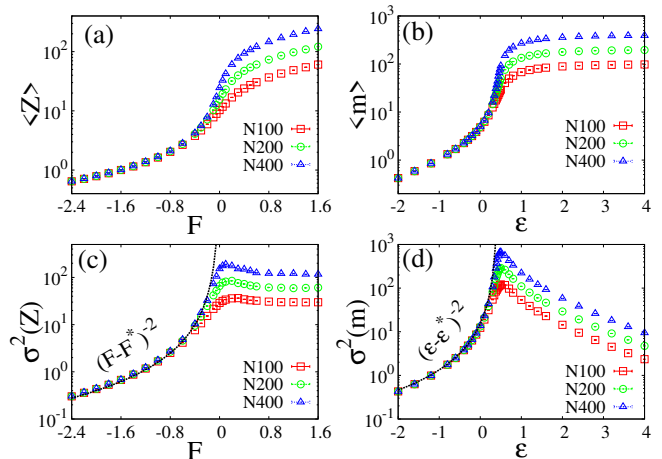


FIG. 4. Non-normalized order parameters $\langle Z \rangle$ (average distance between chain end and surface) and $\langle m \rangle$ (number of monomer contacts with the surface) (a,b) and corresponding fluctuations σ^2 (c,d) as functions of the conjugate variables F (force applied to the chain end) and ε (adsorption strength) for the loop-stretch transition (a,c) and the adsorption transition (b,d) with chain lengths N as indicated. Dashed black lines in (c,d) correspond to a fit of the data for σ^2 below the transition ($F < F^*$ and $\varepsilon < \varepsilon^*$, respectively) to an inverse quadratic law.

tion strength ε . Qualitatively, the curves for the order parameter and its fluctuations show the same behavior. Far below the transition, which corresponds in the loop-stretch case to the loop regime where the direction of F points to the substrate (i.e., negative F values), and in the adsorption case to the regime where the adsorption strength ε is small, the values for the averaged order parameter and its fluctuations coincide for different chain lengths. As the critical point is approached ($F = F^*$ or $\varepsilon = \varepsilon^*$, respectively), they increase and become strongly chain length dependent. After crossing the critical point, the order parameter continues to increase, whereas the fluctuations reach a maximum and then decrease again slowly.

Table I shows the scaling of the quantities under consideration with respect to the chain length N far below the critical point, at the critical point, and above the critical point. Below the critical point, the quantities do not depend on N and scale with the exponent 0. Far above the critical point, they increase linearly with the chain length, i.e., they scale with the exponent 1. At the critical point, the scaling is nontrivial and the exponents differ from each other. In the case of the loop-stretch transition, the scaling of the order parameter Z with chain length roughly corresponds to the Flory exponent $\nu = 0.59$ [31], as one would expect for a force-free single chain in good solvent, and the scaling exponent of the fluctuations is twice that number, $2\nu = 1.18$. The order parameter m of the adsorption transition also scales algebraically with the chain length at the transition point, but with a different exponent $\phi \approx 0.52$ which is approach-

	below	at	above
$\langle Z_1 \rangle$	0 ± 0.002	0.59 ± 0.03	1 ± 0.001
$\langle m \rangle$	0 ± 0.001	0.52 ± 0.01	1.005 ± 0.003
$\sigma^2(Z_1)$	0.01 ± 0.01	1.18 ± 0.02	0.98 ± 0.03
$\sigma^2(m)$	0 ± 0.002	1.06 ± 0.01	1 ± 0.01

TABLE I. Scaling exponents for the quantities in Fig. 4 with chain length N far below the transition ($F = -2.6 \ll F^* = 0$ and $\varepsilon = -2.0 \ll \varepsilon^* = 0.42$), at the transition ($F = F^* = 0.00$ and $\varepsilon = \varepsilon^* = 0.42$), and far above the transition ($F = 1.6 \gg F^*$ and $\varepsilon = 4.0 \gg \varepsilon^*$).

ing 0.5. This exponent will be discussed further below. The scaling exponent characterizing the fluctuations of m is again twice as high, $2\phi \approx 1.06$.

Even though the order parameter and the fluctuations show the same qualitative behavior at the transition, there are quantitative differences: As we have seen above, the critical exponents that characterize the scaling of characteristic quantities with chain length at the transition points are different. Moreover, the comparison of Fig. 4 (c) and (d) suggests that the fluctuations of the order parameter decay much more rapidly above the transition in the case of the adsorption transition than in the case of the loop-stretch transition. Below the transition, however, the behavior of σ^2 at both transitions seems to agree even quantitatively. In both cases, it can be fitted nicely by an inverse quadratic law, $\sigma^2(Z) \sim |F - F^*|^{-2}$ and $\sigma^2(m) \sim |\varepsilon - \varepsilon^*|^{-2}$, and it diverges at the critical point in the infinite chain limit $N \rightarrow \infty$.

It is convenient at this point to discuss separately the near-critical behavior, which will be addressed in the next subsection in the framework of a finite-size scaling theory, and the behavior far away from the critical point. The latter is best understood in terms of thermal “excitations” above the limiting states, which are treated as “ground states”. We first identify the four different “ground states” of our system, akin to the cartoons in Fig. 1 but taken to zero-temperature limit.

- (1) F fixed, $\varepsilon \rightarrow -\infty$: Mushroom state with no surface contacts ($m = 0$)
- (2) F fixed, $\varepsilon \rightarrow +\infty$: Fully adsorbed state, $m = N$
- (3) $F \rightarrow -\infty$, $\varepsilon = 0$: Loop state with $Z = 0$.
- (4) $F \rightarrow +\infty$, $\varepsilon = 0$: Fully stretched state, $Z = N$. This limit cannot be explored in our simulations because of the nature of the model, which does not incorporate finite extensibility.

As long as the excitations are independent modes that can be treated within harmonic approximation, one can apply the equipartition theorem $\langle \Delta E \rangle = \frac{n}{2}$, where n is the number of independent excitation modes, and $\Delta E = \mathcal{H} - E_0$ is the deviation of the energy from the “ground state energy”.

In the extreme cases (1) and (2), the only contribution to the energy comes from the surface contacts ($\langle \Delta E \rangle \sim \varepsilon \langle m \rangle$). In case (1) excitations correspond to isolated contacts bringing positive energy. Since the repulsive contacts are dominated by short subchains originating at the grafting point, the effective number of relevant degrees of freedom is independent of the chain length. In case (2) excitations are associated with local desorption events that can appear along the whole chain, hence n is proportional to the chain length N . This yields immediately $\langle m \rangle \sim |\varepsilon|^{-1}$ in the case (1), and $\langle m \rangle \sim N - N|\varepsilon|^{-1}$ in the case (2). Differentiation with respect to the control parameter ε results in $\sigma^2(m) \sim |\varepsilon|^{-2}$ and $\sigma^2(m) \sim N|\varepsilon|^{-2}$, respectively.

Similarly, in the cases (3,4), the energy is brought by the external end-force: $\langle \Delta E \rangle \sim F \langle Z \rangle$. The excitations are associated with local vertical motions of the pressed end in the loop case (3), and with the full spectrum of elastic modes in the stretched case (4). Hence the number of modes that contribute to the energy is chain length independent in the case (3) and $n \sim N$ in the case (4). One obtains $\langle Z \rangle \sim |F|^{-1}$ and $\sigma^2(Z) \sim \partial \langle Z \rangle / \partial F \sim |F|^{-2}$ in the case (3), and $\langle Z \rangle \sim N - N|F|^{-1}$, $\sigma^2(Z) \sim N|F|^{-2}$ in the case (4).

B. Static critical behavior: Theoretical analysis

The loop-stretch transition has the advantage of allowing a very detailed analytical description of the partition function. We start by summarizing the known results for various partition functions which are naturally formulated in the language of lattice models with well-defined discrete configurations. Since the near-critical behavior of the order parameters is universal, we can eventually apply the theory to our off-lattice simulations. Firstly recall that for a free random walk on a lattice, the total number of distinct walks for N steps is given by

$$Q(N) = \omega^N \quad (3)$$

where ω is the lattice coordination number (e.g., $\omega = 6$ for a cubic lattice). However, for self-avoiding walks of N steps, the total number of walks is smaller, and asymptotically obeys the law

$$Q(N) = \tilde{\omega}^N N^{\gamma-1} \quad (4)$$

where the “connectivity constant” $\tilde{\omega} < \omega$ depends on the dimensionality and the lattice type, and the exponent γ in the “enhancement factor” $N^{\gamma-1}$ depends only on the dimensionality. In three dimensional lattices, one has $\gamma \approx 7/6$ [14].

We consider a real chain, modeled as a self-avoiding walk, which is constrained in half space ($z > 0$) with the one end segment placed at the plane (i.e., at $z = 1$), and define Q_1 as the number of walks which starts from the plane, and Q_{11} as the number of walks which terminates

at the plane. It is reasonable to assume a similar N dependence [32], i.e.,

$$Q_1(N) = \tilde{\omega}^N N^{\gamma_1-1}, \text{ and } Q_{11}(N) = \tilde{\omega}^N N^{\gamma_{11}-1} \quad (5)$$

The values of γ_1 and γ_{11} have been evaluated both by computer simulations and theories [33–36]. According to the recent numerical results from Grassberger and Clisby et al, we take $\gamma_1 \approx 0.68$ and $\gamma_{11} \approx -0.39$ [37–39].

The form of the probability density distribution for the height of the free end was conjectured by Fisher [40]

$$P(Z, N) = \frac{A}{Z_0} \left(\frac{Z}{Z_0}\right)^\theta \exp\left[-B\left(\frac{Z}{Z_0}\right)^\delta\right], \quad (6)$$

where $Z_0 = \langle Z \rangle = bN^\nu$ is the mean end height in the absence of the force, b is a model-dependent prefactor, and the coefficients A and B must be chosen such that $P(Z)$ satisfies the normalization conditions $\int_0^\infty P(Z)dZ = 1$ and $\int_0^\infty dZ Z P(Z) = Z_0$, i.e.,

$$A = \frac{\delta}{\Gamma\left(\frac{1+\theta}{\delta}\right)} \left[\frac{\Gamma\left(\frac{2+\theta}{\delta}\right)}{\Gamma\left(\frac{1+\theta}{\delta}\right)}\right]^{1+\theta}, \quad B = \left[\frac{\Gamma\left(\frac{2+\theta}{\delta}\right)}{\Gamma\left(\frac{1+\theta}{\delta}\right)}\right]^\delta. \quad (7)$$

The exponents δ can be derived from scaling arguments, giving $\delta = \frac{1}{1-\nu}$ [14], and the exponent θ follows from the relation

$$Q_{11} = Q_1 P(Z = 1), \quad (8)$$

which gives

$$N^{\gamma_{11}-1} = N^{\gamma_1-1} Z_0^{-1-\theta} \sim N^{\gamma_1-1-\nu-\nu\theta}, \quad (9)$$

and hence [37]

$$\theta = \frac{\gamma_1 - \gamma_{11} - \nu}{\nu} \simeq 0.8. \quad (10)$$

The coefficients A and B in the distribution function $P(Z, N)$ are completely defined by two critical indices δ and θ with numerical values of $A \approx 1.18$ and $B \approx 0.503$. These results hold for force-free chains that are end-grafted onto a purely repulsive surface ($F = 0$ and $\varepsilon = 0$).

Structurally, the form of $P(Z, N)$ is a natural generalization of the free end probability for an ideal Gaussian chain near an impenetrable plane with ‘‘absorbing’’ boundary conditions [41]. Although the chain end distribution is a common object in polymer theory one should also recognize that in the context of the loop-stretch transition $P(Z, N)$ has the meaning of the order parameter distribution for a finite system at a critical point.

Based on Eq. (6), we express the partition function of a chain subject to an end force F in the force ensemble as

$$Q_F(F, N) = Q_1(N) \int_0^\infty dZ P(Z; N) e^{FZ} = Q_1(N) \Psi_F(FZ_0) \quad (11)$$

with

$$\Psi_F(x) = A \int_0^\infty dt t^\theta \exp\left[-Bt^\delta + xt\right]. \quad (12)$$

and $x = FZ_0$. Hence Q_F has exactly the form assumed in crossover scaling hypothesis

$$Q_F(F, N) = Q_F(F^*) \Psi_F(bFN^\nu), \quad (13)$$

where $F^* = 0$ defines the critical point, Ψ_F is the crossover function which contains all information about the static behavior of the system, and ν acts as a crossover exponent. This is unique case when the crossover function is not just postulated but can be constructed explicitly.

From the analysis of Eq.(12), one can deduce three regimes of crossover behavior. In the limit of $x \ll -1$, the second term in the exponent in Eq.(12) dominates,

$$\Psi_F(x) \sim (-x)^{-\theta-1}. \quad (14)$$

In the vicinity of the transition point, at $x \approx 0$, we can expand e^{xt} , which leads to

$$\Psi_F(x) = 1 + x + c_2 x^2 + \dots, \quad (15)$$

where the coefficient with the linear term equals 1 by normalization conditions, and

$$c_2 = \frac{\Gamma\left(\frac{1+\theta}{\delta}\right)\Gamma\left(\frac{3+\theta}{\delta}\right)}{2\left(\Gamma\left(\frac{2+\theta}{\delta}\right)\right)^2} \quad (16)$$

Numerically, $c_2 \approx 0.63$.

In the large force limit $x \gg 1$, the integrand in Eq.(12) becomes very sharp, and we can carry out a saddle point approximation about the saddle point $t_c = \left(\frac{x}{B\delta}\right)^{\frac{1}{\delta-1}}$, giving

$$\Psi_F(x) \sim \exp(Cx^{1/\nu}) \quad (17)$$

where $C = \nu\left(\frac{1-\nu}{B}\right)^{\frac{1-\nu}{\nu}} = 0.51$. Together, we obtain

$$\ln \Psi_F(x) \approx \begin{cases} -(1+\theta) \ln(-x), & x \ll -1 \\ x + (c_2 - \frac{1}{2})x^2, & |x| \ll 1 \\ Cx^{1/\nu}, & x \gg 1 \end{cases} \quad (18)$$

We note that in the pre-transitional regime not only the logarithmic shape itself but also the numerical prefactor $(1+\theta)$ is predicted to be model-independent. The shape of the crossover function $\ln \Psi_F(x)$ is shown in Fig. 5 together with the two main asymptotics. In the stretching regime the logarithm of the exact crossover function differs from the asymptotic branch by a constant shift which does not affect the behavior of the observables.

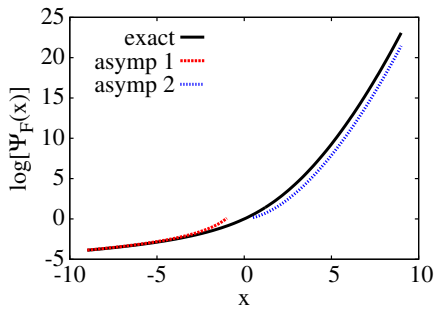


FIG. 5. Logarithm of the crossover function of the loop-stretch transition together with two asymptotic curves for the loop regime (1) and the stretch regime (2)

Knowing the crossover function $\Psi_F(x)$, the asymptotic behavior of the average height can be evaluated according to $\langle Z \rangle = \frac{\partial \ln \Psi_F(FN^\nu)}{\partial F}$, which leads to

$$\langle Z \rangle \sim \begin{cases} \frac{1}{F^* - F}, & x \ll -1 \\ N^\nu, & |x| \ll 1 \\ N(F - F^*)^{\frac{1-\nu}{\nu}}, & x \gg 1 \end{cases} \quad (19)$$

Similarly, the asymptotic behavior of the height fluctuations is given by $\sigma^2(Z) = \langle Z^2 \rangle - \langle Z \rangle^2 = \frac{\partial^2 \ln \Psi_F(FN^\nu)}{\partial F^2}$, leading to

$$\sigma^2(Z) \sim \begin{cases} \frac{1}{(F - F^*)^2}, & x \ll -1 \\ N^{2\nu}, & |x| \ll 1 \\ N(F - F^*)^{\frac{1-2\nu}{\nu}}, & x \gg 1. \end{cases} \quad (20)$$

All theoretical predictions are in good agreement with the simulation data presented in the previous subsection, Fig. 4(a) and (c). A more detailed comparison will follow below.

Next we consider the desorption-adsorption transition. A finite-size scaling hypothesis for the partition function $Q_\varepsilon(\varepsilon, N)$ of the adsorbing chain in a vicinity of the critical point, similar to Eq. (13), was proposed on the basis of the polymer-magnetic analogy [15, 37, 42–44]:

$$Q_\varepsilon(\varepsilon, N) = Q_\varepsilon(\varepsilon^*, N) \Psi_\varepsilon[(\varepsilon - \varepsilon^*)N^\phi], \quad (21)$$

where ϕ is the crossover exponent for critical adsorption, which has been discussed extensively in the literature [15, 37, 42–44]. According to recent extensive lattice simulations, the value of the crossover exponent ϕ is given by $\phi = 0.483 \pm 0.003$ [37, 44]. At chain lengths comparable to the ones used in the present study, one typically observes higher apparent exponent close to $\phi = 0.5$. [44].

The crossover function $\Psi_\varepsilon(x)$ gives the average contact number $\langle m \rangle = \frac{\partial \ln \Psi_\varepsilon((\varepsilon - \varepsilon^*)N^\phi)}{\partial \varepsilon}$. Traditionally, the asymptotic behavior of $\Psi_\varepsilon(x)$ where $x = (\varepsilon - \varepsilon^*)N^\phi$ is reconstructed from the expected asymptotic behavior of $\langle m \rangle$.

- In the fully developed adsorption regime $x \gg 1$, the number of adsorbed monomers is proportional to N , $m \sim N$. Hence, one should have $\ln(\Psi_\varepsilon(x)) \sim x^{1/\phi}$ in this limit.
- The crossover function is analytic at the transition point $x = 0$, therefore it can be Taylor expanded for $|x| \ll 1$ giving $\Psi_\varepsilon(x)$ as $\Psi_\varepsilon(x) = 1 + c'_1 x + c'_2 x^2 + \dots$
- For strong enough repulsion $x \ll -1$, very few monomers are contacting the substrate, therefore $\langle m \rangle$ should be independent of N . In this limit, $d \ln(\Psi_\varepsilon(x))/dx$ should thus scale like $1/x$, hence $\ln(\Psi_\varepsilon(x)) \sim \ln(-x)$.

With these consideration, we summarize the asymptotic expressions of $\Psi_\varepsilon(x)$ as

$$\ln \Psi_\varepsilon(x) \sim \begin{cases} \ln(-x), & x \ll -1 \\ c'_1 x + c'_2 x^2, & |x| \ll 1 \\ x^{1/\phi}, & x \gg 1, \end{cases} \quad (22)$$

and obtain for the average contact number

$$\langle m \rangle \sim \begin{cases} \frac{1}{\varepsilon^* - \varepsilon}, & x \ll -1 \\ N^\phi, & |x| \ll 1 \\ N(\varepsilon - \varepsilon^*)^{\frac{1-\phi}{\phi}}, & x \gg 1. \end{cases} \quad (23)$$

The fluctuations of m are calculated as $\sigma^2(m) = \langle m^2 \rangle - \langle m \rangle^2 = \frac{\partial^2 \ln \Psi_\varepsilon((\varepsilon - \varepsilon^*)N^\phi)}{\partial \varepsilon^2}$, yielding

$$\sigma^2(m) \sim \begin{cases} \frac{1}{(\varepsilon^* - \varepsilon)^2}, & x \ll -1 \\ N^{2\phi}, & |x| \ll 1 \\ N(\varepsilon - \varepsilon_c)^{\frac{1-2\phi}{\phi}}, & x \gg 1, \end{cases} \quad (24)$$

which is in qualitative agreement with Fig. 4 (c) and (d) if one assumes $\phi = 0.52$.

Earlier we have seen that this type of asymptotic behavior of the crossover function follows naturally from its connection to a specific shape of the probability density for the order parameter at the transition point. Thus we propose a Fisher-type conjecture, see Eq. (6) for the distribution of the number of contacts at the critical adsorption point.

$$P(m, N) = \frac{A'}{m_0} \left(\frac{m}{m_0} \right)^{\theta'} \exp \left[-B' \left(\frac{m}{m_0} \right)^{\frac{1}{1-\phi}} \right]. \quad (25)$$

Here $m_0 = \langle m \rangle = b'N^\phi$ is the average number of contacts at the critical point, b' is a model-dependent prefactor, index δ' is related to the crossover exponent as $\delta' = (1 - \phi)^{-1}$, and θ' is yet another exponent describing the probabilities of chain conformations with very few contacts at critical conditions $\varepsilon = \varepsilon^*$. The coefficients A' and B' are determined by normalization and expressed in terms of the exponents θ' and δ' according to Eq.(7).

Following the discussion around Eqs.(8)-(10) we write

$$Q_{11} = Q_{11c} P(m = 1), \quad (26)$$

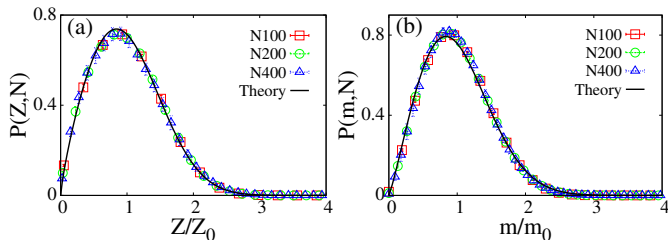


FIG. 6. Rescaled order parameter distribution at the critical point for the loop-stretch transition (a) (at $\varepsilon = 0$) and the adsorption transition (b) (at $F = -2$) for different chain lengths as indicated, compared to the predictions of the theoretical conjectures Eq. (6) with exponents $\theta = 0.8$ and $\nu = 0.58$ in (a) and Eq. (25) with exponents $\theta' = 1.1$ and $\phi = 0.52$ in (b).

where

$$Q_{11c}(N) = \tilde{\omega}^N N^{\gamma_{11c}-1} \quad (27)$$

is the partition function of the loop at the critical adsorption point, and γ_{11c} is the corresponding surface exponent. Numerically, $\gamma_{11c} \approx 0.707$ [37]. Equation (26) leads to

$$\theta' = \frac{\gamma_{11c} - \gamma_{11} - \phi}{\phi} \simeq 1.1 \quad (28)$$

in full analogy to Eq. (10). We test the conjectures (6) and (25) by comparing them with the corresponding order parameter distributions at the respective critical conditions as obtained from the simulations. The results are shown in Fig. 6. If plotted as a function of the relevant scaling variable, Z/Z_0 , and m/m_0 , the theoretical predictions as well as the distribution functions for different chain lengths obtained from simulations collapse almost perfectly. Note that theoretical conjectures contain no fitting parameters at all.

From Eq. (25), we can construct the adsorption crossover function $\Psi_\varepsilon(x)$ according to Eq. (12) with proper replacement of the parameters, leading to a similar form:

$$\Psi_\varepsilon(x) = A' \int_0^\infty dt t^{\theta'} \exp[-B' t^{\delta'} + xt] \quad (29)$$

where $x = (\varepsilon - \varepsilon^*)m_0 = b'(\varepsilon - \varepsilon^*)N^\phi$. According to this equation, the differences between the equilibrium near-critical behavior at the loop-stretch and the loop adsorption transitions for large chain lengths, $N \rightarrow \infty$, can thus be traced back to the differences in the pair of exponents, of which one (θ, θ') shows up directly in the amplitude of the pre-translational branch. The post-translational growth of the order parameter is directly affected by the crossover exponents, ν and ϕ , respectively, and indirectly (through the coefficients B) by the value of the θ exponent. Interestingly, the crossover exponents are rather close numerically while the other pair differ more considerably. We shall see, though, that the width of the near-critical scaling region in terms of the respective control parameters (F and ε) is dramatically smaller for the loop adsorption.

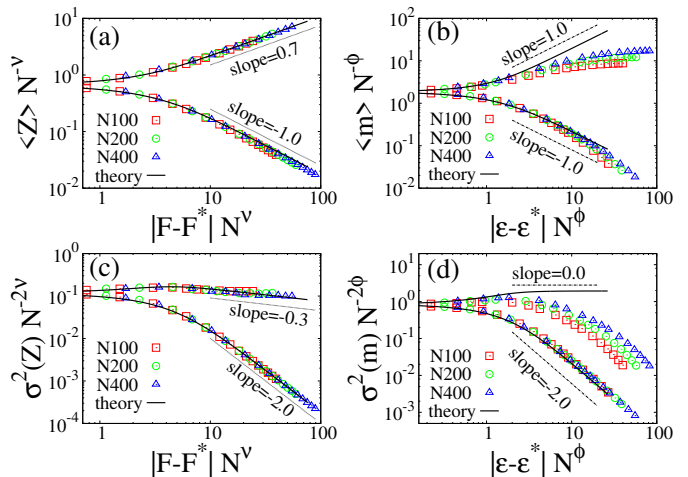


FIG. 7. Same data as Fig. 4, rescaled as suggested by Eqs. (30) (a,c) and (31) (b,d). Lower branch indicates the regime below the critical point ($F < F^* = 0$ and $\varepsilon < \varepsilon^* = 0.42$, respectively), and upper branch the regime above the critical point ($F > F^*$ and $\varepsilon > \varepsilon^*$, respectively). Black solid lines represent the predictions of the explicit crossover function. Dashed lines show asymptotically expected slopes far from the transition, if one assumes that the order parameters and their fluctuations scale like N^0 in the lower branch, and like N^1 in the upper branch.

C. Simulation results in the finite-size scaling framework

According to the analysis developed in the last subsection for the loop-stretch transition, the results for $\langle Z \rangle$ and $\sigma^2(Z)$ can also be written in a scaling form,

$$\begin{aligned} \langle Z \rangle &= N^\nu \hat{f}_Z((F - F^*)N^\nu), \\ \sigma^2(Z) &= N^{2\nu} \hat{f}_{\sigma_Z^2}((F - F^*)N^\nu), \end{aligned} \quad (30)$$

where the scaling functions $\hat{f}_Z(x) \propto d \ln \Psi_F(x)/dx$ and $\hat{f}_{\sigma_Z^2}(x) \propto d^2 \ln \Psi_F(x)/dx^2$ show asymptotic scaling behavior $\hat{f}(x) \sim (\pm x)^{\alpha_\pm}$ for large $\pm x \gg 1$ with exponents $\alpha_- = -1$ and $\alpha_+ = 1/\nu - 1 \approx 0.7$ for \hat{f}_Z , and $\alpha_- = -2$, $\alpha_+ = 1/\nu - 2 \approx -0.3$ for $\hat{f}_{\sigma_Z^2}$. This implies that the curves of $\langle Z \rangle$ and $\sigma^2(Z)$ for different chain lengths N should collapse, if we plot $\langle Z \rangle N^{-\nu}$ and $\sigma^2(Z) N^{-2\nu}$ as a function of the scaling variable $x \sim (F - F^*)N^\nu$. The rescaled data are displayed in Fig. 7(a) and (c) together with theoretical curves evaluated from the explicit crossover function of Eq. (12) with the numerical value $b = 0.66$ taken from simulations. Indeed, the data collapse nicely, and are in perfect agreement with the theoretical curves.

In the same vein, the data of Fig. 4 (c,d) should collapse onto one curve if one plots $\langle m \rangle N^{-\phi}$ and $\sigma^2(m) N^{-2\phi}$ as a function of the scaling variable $x = (\varepsilon - \varepsilon^*)N^\phi$. More specifically, the results (23) and (24) can be rewritten in a scaling form

$$\langle m \rangle = N^\phi \hat{f}_m((\varepsilon - \varepsilon^*)N^\phi), \quad (31)$$

$$\sigma^2(m) = N^{2\phi} \hat{f}_{\sigma_m^2}((\varepsilon - \varepsilon^*)N^\phi),$$

where the scaling functions $\hat{f}_m(x) \propto d \ln \Psi_\varepsilon(x)/dx$ and $\hat{f}_{\sigma_m^2}(x) \propto d^2 \ln \Psi_\varepsilon(x)/dx^2$ show asymptotic scaling behavior $\hat{f}(x) \sim (\pm x)^{\alpha_\pm}$ for large $\pm x \gg 1$ with $\alpha_- = -1$ and $\alpha_+ = 1/\phi - 1 \approx 1$ for \hat{f}_m , and $\alpha_- = -2$, $\alpha_+ = 1/\phi - 2 \approx 0$. for $\hat{f}_{\sigma_m^2}$. The rescaled data are shown in Fig. 7 (b) and (d), together with the theoretical curve derived from Eq. (29) with the numerical value $b' = 1.85$ taken from simulations. Even though ϕ has been adjusted to optimize the collapse, the data collapse is not nearly as good as in the case of the loop-stretch transition. The best collapse is obtained for $\phi = 0.52$, which is consistent with the scaling suggested by Fig. 6 and close to the literature value, $\phi \approx 0.483$ [37, 44]. In the near-critical regime, the theoretical curves obtained from the conjectured explicit form of the crossover function, Eq. (29), compare well with the simulation data.

However, at some distance from the transition, the curves for different N do not collapse and the asymptotic behavior of the curves does not reproduce the theoretically predicted slopes for the chain lengths under consideration. The main reason for these deviations is that the near-critical behavior at adsorption is apparently restricted to a rather narrow range of the adsorption parameter ε near ε^* . For stronger adsorption, saturation effects start suppressing the power-law growth of the contact numbers which leads to a corresponding decrease in their fluctuations. This phenomenon falls outside the crossover Ansatz; deviations, however, cannot be seen at the level of the probability density of Fig. 6 as they pertain to the far-off tail at large values of the order parameter.

D. Dynamical behavior

After studying the static critical behavior, we turn our attention to the dynamic behavior of the order parameters. Relaxation of the free end for a chain grafted to a repulsive surface was never studied in the context of the loop-stretch transition. As for the relaxation of the number of contacts, it was evaluated only at the critical point of adsorption in [43]. We calculate the autocorrelation function of the two order parameters, i.e., $C_Z(t) = \frac{\langle Z(t)Z(0) \rangle - \langle Z \rangle^2}{\sigma^2(Z)}$ and $C_m(t) = \frac{\langle m(t)m(0) \rangle - \langle m \rangle^2}{\sigma^2(m)}$, from which the characteristic relaxation times $\tau(Z) = \int_0^\infty dt C_Z(t)$ and $\tau(m) = \int_0^\infty dt C_m(t)$ can be evaluated. The results are presented in Fig. 8.

Below the phase transition, for negative forces or non-adsorbing surfaces, respectively, the relaxation times show a similar behavior at the two transitions. They are almost independent of chain length and increase as the critical point is approached. Close to the critical point, they become strongly chain length dependent and develop a maximum, which would diverge in the limit $N \rightarrow \infty$. (Note that the maximum in the case of the loop-

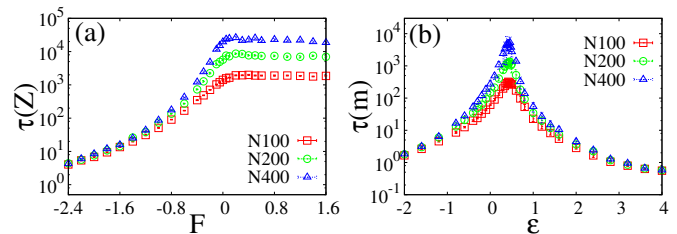


FIG. 8. Characteristic relaxation times of the order parameter Z (chain end position), $\tau(Z)$, and m (number of monomer contacts with the surface), $\tau(m)$, as functions of the respective control parameters F (force applied to the chain end) and ε (adsorption strength) (a) at the loop-stretch transition ($\varepsilon = 0$), and (b) at the loop adsorption transition ($F = -2$) and different chain lengths as indicated.

	below	at	above
$\tau(Z)$	0.07 ± 0.06	2.18 ± 0.12	1.86 ± 0.14
$\tau(m)$	0.02 ± 0.01	2.05 ± 0.03	0.03 ± 0.01

TABLE II. Scaling exponents α for the N -dependence $\tau \sim N^\alpha$ of the two relaxation times $\tau(Z)$ and $\tau(m)$ in Fig. 8 far below the transition ($F = -2.6 \ll F^*$ and $\varepsilon = -2.0 \ll \varepsilon^*$), at the transition ($F = F^* = 0.00$ and $\varepsilon = \varepsilon^* = 0.42$), and far above the transition ($F = 1.6 \gg F^*$ and $\varepsilon = 4.0 \gg \varepsilon^*$).

stretch transition is much less prominent but still exists). Above the transition, however, the curves in Figs. 8(a) and (b) are markedly different. In stretched chains, the relaxation times remain large and still depend strongly on the chain length, whereas in adsorbed chains far above the adsorption point, they drop down again and become roughly chain length independent. This is also apparent from Table II, which shows the scaling of τ with the chain length $\tau \sim N^\alpha$, far from the transition and at the transition. Far below the transition, one has $\alpha = 0$ both for the loop-stretch and the adsorption transition. At the transition, the scaling exponent α is nontrivial and close to 2 in both cases. Far above the transition, one recovers $\alpha = 0$ in the adsorption case, whereas α settles at $\alpha = 2$ in the loop-stretch case.

To quantify the global relaxation in the case of the loop-stretch transition, one can introduce an effective longitudinal diffusion coefficient D , which characterizes the motion of an “equivalent” single particle in a harmonic potential chosen such that the variance $\sigma^2(Z)$ is the same. From the theory of Brownian motion, the effective diffusion constant can be estimated by $D = \frac{\sigma^2(Z)}{2\tau(Z)}$ [45]. The results for D are presented in Fig. 9(a). Here, the variance $\sigma^2(Z)$ is obtained directly from the trajectory of the free end, and the relaxation time $\tau(Z)$ is calculated from the autocorrelation functions. Below the loop-stretch transition, for negative forces F , D decreases as the transition is approached. In the transitional regime as well as for the stretched coil, the diffusion coefficient

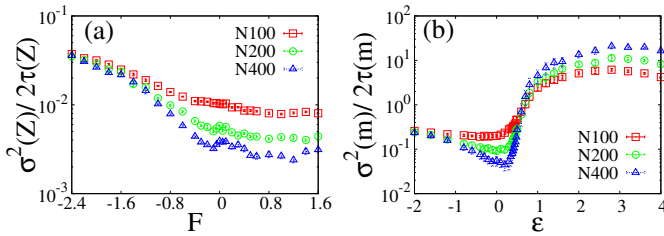


FIG. 9. (a) Effective diffusion coefficient $D = \sigma^2(Z)/2\tau(Z)$ of the chain end as a function of applied force F . Panel (b) shows the corresponding quantity for m , which has the meaning of the effective frequency of monomer adsorption-desorption events.

roughly recovers the Rouse scaling law for a free draining chain $D \sim N^{-1}$. Since the inverse diffusion constant, $1/D$, corresponds to a friction, one can conclude that all chain monomers contribute to the effective friction of stretched chains, whereas only a fraction contributes for chains with ends pressed towards the surface. Over all, however, the variations of D are relatively small. The effective diffusion constant does not change by orders of magnitude.

In the case of the adsorption transition, an analysis in terms of an effective diffusion constant (and corresponding friction) is less straightforward. However, one can imagine the relaxation process as a sequence of more or less correlated monomer adsorption/desorption events. Each event changes the number of contacts by ± 1 . Taking this as an uncorrelated random walk along m axis with t_0 as the time per single step we obtain for the mean-square displacement as a function of time $\langle(\Delta m)^2(t)\rangle = t/t_0$. Hence, the relaxation time scales as $\tau(m) \sim t_0 \sigma^2(m)$, and the ratio $\sigma^2(m)/\tau(m)$ has the meaning of the effective frequency t_0^{-1} of the adsorption-desorption steps. The fact that at strong adsorption this frequency is proportional to N , see Fig. 9 (b), means that the steps happen independently at different locations along the chain and are, indeed, weakly correlated. In the near-critical region these steps appear to be strongly correlated leading a very low effective frequency $\sim N^{-1}$. At strong repulsion, the frequency increases again since the correlations are now limited to a fairly small part of the chain adjacent to the grafting point. Overall the variation of frequency t_0^{-1} in the adsorption transition is much stronger than that of the diffusion coefficient D in the loop-stretch transition and shows a non-monotonic behavior.

In the static case, we had established a formal analogy between the adsorption and the loop-stretch transition in Sec. III B. It was based on the same form of the probability distributions for the order parameter at the critical point leading to the crossover functions Ψ_F and Ψ_ε (Eqs. (18) and (22)) of the same structure. However, the underlying Hamiltonian does not have this symmetry. The Hamiltonian of a strongly stretched end-grafted chain at $\varepsilon = 0$ can be approximated by that of an

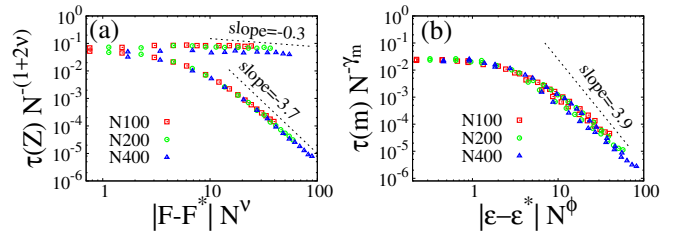


FIG. 10. Same data as Fig. 8 rescaled according to Eq. (32) with $\gamma_Z \approx 1 + 2\nu$ (a) and Eq. (33) with $\gamma_m = 2.05$ (b). Lower branch in (a) and upper branch in (b) correspond to the regime below the transition, upper branch in (a) and lower branch in (b) to the regime above the transition.

ideal free stretched chain; all monomer-monomer correlations and their relaxation are determined by the normal modes, and the relaxation mechanism is essentially diffusive. The fact that the relaxation time $\tau(Z)$ scales as $\tau \sim N^2$ for strongly stretched chains indicates a typical Rouse behavior [25]. The case of a strongly adsorbed chain at $F = 0$ is quite different, since both the attractive and the repulsive part of the surface interaction play essential roles. Diagonalization of the Hamiltonian is not possible. Pair correlation functions for monomers separated by a large contour distance (larger than the adsorption blob size), are suppressed, and thus large-scale relaxations do not contribute to time correlation function of the monomer-surface contact number, $\langle m(0)m(t) \rangle$.

To further analyze the dynamic scaling behavior of the order parameters of the loop-stretch and adsorption transition, we again make a scaling Ansatz, similar to (30) and (31).

$$\tau(Z) = N^{\gamma_Z} \hat{f}_{\tau_Z}[(F - F^*)N^\nu] \quad (32)$$

$$\tau(m) = N^{\gamma_m} \hat{f}_{\tau_m}[(\varepsilon - \varepsilon^*)N^\phi] \quad (33)$$

For free chains, the characteristic relaxation time of the end-to-end distance is expected to scale as $\tau \sim N^{1+2\nu}$ (in the absence of hydrodynamics) [25]. It seems reasonable to assume that this exponent also sets the exponent γ_Z in Eq. (32), i.e., one expects $\gamma_Z = 1 + 2\nu = 2.18$. Indeed, this exponent is compatible with the scaling of τ with chain length at the loop-stretch transition (Table II), and Fig. 10(a) demonstrates that the data of Fig. 8(a) for different chain lengths collapse nicely onto one curve if they are rescaled as suggested by Eq. (32) with this exponent. For large negative F (strongly pressed chain ends), the relaxation of Z is dominated by local processes close to the end monomer and expected to be independent of the total chain length (see also Table II). Thus one expects the scaling function \hat{f}_{τ_Z} to scale as $\hat{f}_{\tau_Z}(x) \sim x^{-1/\nu-2} \sim x^{-3.7}$, which is roughly compatible with the data in Fig. 10(a) (lower branch). For large positive F (strongly stretched chain), the effective diffusion constant scales as $D \sim 1/N$ as discussed above, hence $\hat{f}_{\tau_Z}(x)$ must show the same scaling behavior with x than $\hat{f}_{\sigma^2(Z)}(x)$, $\hat{f}_{\tau_Z} \sim x^{1/\nu-2} \sim x^{-0.3}$, which is also compatible

with Fig. 10(a) (upper branch).

Since $\tau \sim N^{1+2\nu}$ sets a characteristic time scale for grafted chains in general, one might expect that it also characterizes the relaxation time of the adsorption process [43], which would imply $\gamma_m = \gamma_Z = 2.18$. However, the simulation data for $\tau(m)$ at different chain lengths do not collapse if they are rescaled with that exponent (data not shown). Moreover, right at the transition, $\tau(m)$ was found to scale with N with the exponent 2.05 ± 0.03 (see Table II), which suggests $\gamma_m \approx 2.05$. Rescaling the data with this exponent, one obtains good data collapse (see Fig. 10 (b)). Far from the transition, the relaxation time is found to be chain length independent both for $\varepsilon \ll \varepsilon^*$ and $\varepsilon \gg \varepsilon^*$, which implies that the scaling function $\hat{f}_{\tau(m)}$ should scale as $N^{-\gamma_m/\phi} \sim N^{-3.9}$. Fig. 10 (b) indicates that $\hat{f}_{\tau(m)}(x)$ indeed approaches this scaling for very large arguments $|x|$.

It is clear that even within the error, γ_m is still smaller than $1 + 2\nu$ which is expected to be the only characteristic time scale for grafted chains. We do not have a good explanation for this observed difference. At the adsorption critical point, the dynamics should be fully coupled, which precludes two different global relaxation times with a different N scaling. On the other hand, Fig. 8 shows that the characteristic time scales $\tau(Z)$ and $\tau(m)$ are quite different even at the same state point ($F = 0, \varepsilon = 0$). Previous authors have also reported discrepancies in the quality of the dynamic scaling of $\tau(Z)$ and $\tau(m)$ [43]. It seems conceivable that the coupling of the dynamics of the order parameters Z and m is weak, such that the slower relaxation time (with scaling N^{γ_Z}) only dominates in the limit of very long chains.

IV. SUMMARY

To summarize, we have investigated the critical behavior of the loop-stretch transition of end-grafted chains on neutral substrates by Brownian Dynamics simulations and compared it with the critical behavior at the adsorption transition of a loop. Loop adsorption was chosen to avoid possible complications due to multicritical phenomena in the standard adsorption transition of a single grafted chain.

We describe the loop-stretch transition in terms of the order parameter $\langle Z \rangle$, the average height of the free end, and the adsorption transition in terms of the order parameter $\langle m \rangle$, the average number of adsorbed segments. Both the analytical theory and the numerical results suggest that the thermodynamic behavior of these two order parameters is formally identical, with the same scaling with chain length, if one replaces the crossover exponent ϕ in the adsorption transition by the Flory exponent ν in the loop-stretch transition, and the crossover variable $x = (\varepsilon - \varepsilon^*)N^\phi$ (in the adsorption transition) by $x = (F - F^*)N^\nu$ (in the loop-stretch transition) (cf. Eqs. (18) and (22)).

We show that both transitions provides a rare opportunity to study in detail a continuous phase transition with the crossover behavior characterized by two non-trivial critical exponents with an explicit analytical form of the crossover function. This exceptional situation is made possible by a Fisher Ansatz [40] proposed for distribution of the free end position for a chain end-grafted to a non-adsorbing surface. Recognizing this as the order parameter distribution at the critical point of the loop-stretch transition we extend the Ansatz to cover the loop adsorption transition as well. In both cases, the order parameter distribution is characterized by a pair of indices one of which is strictly defined by the relevant crossover exponent (ν or ϕ) while the other is also related to a pair of the partition function surface exponents (γ_1, γ_{11}) or ($\gamma_{11c}, \gamma_{11}$), respectively. No fitting parameters are involved in the scaling form of the order parameter distribution function. Explicit crossover function follows from Boltzmann re-weighting of the order parameter distribution and provides an excellent agreement with the simulation results within the near-critical domain.

On the other hand, the dynamic relaxation behavior of the two order parameters shows significant differences especially above the transition. While the relaxation behavior for Z above the loop-stretch transition shows a typical Rouse behavior with relaxation times scaling as $\tau(Z) \sim N^2$, the relaxation time for m decays rapidly above the adsorption transition and becomes essentially independent of the chain length far from the critical point, i.e., the adsorption dynamics is local as in an Ising model. Right at the critical point, critical slowing down is observed in both cases. The dynamic critical behavior at the adsorption transition is compatible with a scaling Ansatz with crossover variable $x = (\varepsilon - \varepsilon^*)N^\phi$, however, the scaling exponent γ right at the transition ($\tau(m)|_{\varepsilon^*} \sim N^\gamma$) is smaller than the theoretically expected value $\gamma = 1 + 2\nu$. Likewise, the dynamic critical behavior at the loop-stretch transition is described very well by a scaling Ansatz with crossover variable $x = (F - F^*)N^\nu$ and in this case, the scaling exponent takes the expected value, $\gamma = 1 + 2\nu$.

To our best knowledge, the critical behavior of non-ideal chains at the loop-stretch transition has been investigated for the first time in the present work. Based on a conjecture by Fisher, we have derived an analytical expression for the crossover function in the scaling hypothesis for the behavior at finite N , which is in excellent quantitative agreement with our simulation data. We have generalized the Fisher conjecture to be applied to the order parameter distribution of the loop adsorption transition, and demonstrated that it provides an excellent description of the near-critical scaling regime. We believe that this approach could be further extended to cover continuous transitions provided the order parameter is non-negative and interfacial phenomena do not interfere in the ordered state. Coil-globule transition in a flexible chain could be a tentative candidate belonging to this class.

ACKNOWLEDGMENTS

This work has been supported by the German Science Foundation (DFG) within the Graduate School of Excellence Materials Science in Mainz (MAINZ), the grant Schm 985/13-2, the grant NNIO-a 17-53-1213, and the SFB TRR 146 (project C1). D.Y. acknowledges financial support from the National Natural Science Foundation of China (NSFC) 21374011, 21434001. Simulations were carried out on the computer cluster Mogon at JGU Mainz.

Appendix A: Brownian dynamics scheme

In this Appendix we describe the simulation method in detail. We adopt the over-damped Brownian dynamics to propagate the system (see Eq.(2)). The system Hamiltonian is composed by two parts, i.e., $\mathcal{H} = \mathcal{H}_0 + \mathcal{H}_1$, where \mathcal{H}_0 represents the contribution from the chain connection, while \mathcal{H}_1 is the interaction part. To be more general we write the interaction part as a continuous integral

$$\mathcal{H}_1 = \frac{v}{2} \int d\mathbf{r} \hat{\rho}^2(\mathbf{r}) - \varepsilon \int d\mathbf{r} U_a(\mathbf{r}) \hat{\rho}(\mathbf{r}) \quad (\text{A1})$$

where the first term on the right hand side describes the excluded volume interaction, while the second term is adsorption energy. The above Hamiltonian corresponds to the system with pure adsorption, in the following we focus mainly on the adsorption system. In the case of pure stretching, one could directly add the stretching force to the first bead and remove the adsorption force. The density operator at present can be defined as a delta function $\hat{\rho}(\mathbf{r}) = \sum_j \delta(\mathbf{r} - \mathbf{R}_j)$, where the bead index j runs over all beads. By performing the derivative and using the chain rule, we obtain

$$\frac{\partial \mathcal{H}}{\partial \mathbf{R}_j} = 3(2\mathbf{R}_j - \mathbf{R}_{j+1} - \mathbf{R}_{j-1}) + \frac{\partial}{\partial \mathbf{R}_j} [v\hat{\rho} - \varepsilon U_a] \quad (\text{A2})$$

where j is valid for any intermediate beads. The first bead $j = 1$ is only connected to the second bead, while for the last bead $j = N$, it is always fixed at the grafting point. By introducing a potential $\hat{\omega} \equiv v\hat{\rho} - \varepsilon U_a$, the BD equation for the first bead is written as

$$\frac{d\mathbf{R}_1}{dt} = 3(\mathbf{R}_2 - \mathbf{R}_1) - \frac{\partial \hat{\omega}(\mathbf{R}_1)}{\partial \mathbf{R}_1} + \sqrt{2}\mathbf{f}_r, \quad (\text{A3})$$

for the bead $j = N$, $\frac{d\mathbf{R}_N}{dt} = 0$, for any bead $1 < j < N$

$$\frac{d\mathbf{R}_j}{dt} = 3(\mathbf{R}_{j+1} + \mathbf{R}_{j-1} - 2\mathbf{R}_j) - \frac{\partial \hat{\omega}(\mathbf{R}_j)}{\partial \mathbf{R}_j} + \sqrt{2}\mathbf{f}_r. \quad (\text{A4})$$

In order to proceed, we need an explicit expression for the potential derivative. Since the potential is directly determined by the bead density, the evaluation of its derivative is coupled to the way of assignment of particle-to-mesh

density. In practice, we divide the simulation box uniformly into $n_x \cdot n_y \cdot n_z$ cells. All the quantities are defined at the center of each cell, and we call these center points as mesh points. Each cell has a volume of $\Delta V = l_x \cdot l_y \cdot l_z$. In the simulation we chose $l_x = l_y = l_z = a$, meaning that each cell has a unit volume. Therefore the mesh points are located at $x = 0.5 + ml_x$, $y = 0.5 + nl_y$, $z = 0.5 + ol_z$, where the integers $m \in [0, n_x - 1]$, $n \in [0, n_y - 1]$, $o \in [0, n_z - 1]$. Fractions of a bead are assigned to its neighbouring mesh points according to the predefined assignment function $g(\mathbf{r})$ depending only on the distance between the particle and mesh point. Rather than choosing g as a delta function in the continuum case, in practice g has a finite width playing the role of a smear function (or coarse-graining function).

In terms of this assignment function, the density operator can be written as $\hat{\rho}(\mathbf{r}_g) = \frac{1}{\Delta V} \sum_j g(|\mathbf{R}_j - \mathbf{r}_g|)$, where \mathbf{r}_g denotes the position of the g th mesh point. Now we can write \mathcal{H}_1 in a discretized form

$$\mathcal{H}_1 = \frac{v}{2} \Delta V \sum_g \hat{\rho}^2(\mathbf{r}_g) - \Delta V \varepsilon \sum_g U_a(\mathbf{r}_g) \hat{\rho}(\mathbf{r}_g) \quad (\text{A5})$$

which is equivalent to the corresponding interaction energy in Eq.(1) as $\Delta V = 1$. Then the derivative of \mathcal{H}_1 can be performed to get

$$\frac{\partial \mathcal{H}_1}{\partial \mathbf{R}_j} = \frac{\partial \hat{\omega}}{\partial \mathbf{R}_j} = \sum_g \hat{\omega}(\mathbf{r}_g) \frac{\partial}{\partial \mathbf{R}_j} g(|\mathbf{R}_j - \mathbf{r}_g|) \quad (\text{A6})$$

To perform the derivative of the assignment function, we need its explicit expression. For such a purpose, we consider the mesh in which \mathbf{R}_j is located. There are totally eight vertexes for the mesh, and let i, j, k denote the indices along x, y, z directions, respectively. This means that $i = 0, j = 0, k = 0$ mark the vertex number 0 with coordinate $(0, 0, 0)$; $i = 0, j = 0, k = 1$ is the vertex number 1 with coordinate $(0, 0, l_z)$, $i = 0, j = 1, k = 0$ is the vertex number 2 with coordinate $(0, l_y, 0)$, and so on until $i = 1, j = 1, k = 1$ is the the vertex number 7 with coordinate (l_x, l_y, l_z) . Within this mesh, the j th bead is located at $\mathbf{R}_j = (X, Y, Z)$. There are several choices for the assignment function. The lowest order scheme is to assign each bead to its nearest mesh point, and this is called the nearest-grid-scheme. Here we use a higher order scheme, which assigns a fraction of bead to each of its eight nearest mesh points. The fraction assigned to a given vertex is proportional to the volume of a rectangle whose diagonal is the line connecting the particle position and the mesh point on the opposite side of the mesh cell. With the precise arrangement of vertexes, the assignment function for each vertex can be written as

$$g(\mathbf{R}_j - \mathbf{r}_g) = \frac{(l_x - |r_{gx} - X|)(l_y - |r_{gy} - Y|)(l_z - |r_{gz} - Z|)}{l_x l_y l_z} \quad (\text{A7})$$

where g ranges from 0 to 7, $r_{g\alpha}$ is the α component of \mathbf{r}_g . Performing the derivative of the assigning function

directly, we obtain

$$\begin{aligned} \frac{\partial \hat{\omega}}{\partial R_{jx}} &= \frac{\hat{\omega}(\mathbf{r}_4) - \hat{\omega}(\mathbf{r}_0)}{l_x} \frac{(l_y - Y)(l_z - Z)}{l_y l_z} \\ &+ \frac{\hat{\omega}(\mathbf{r}_5) - \hat{\omega}(\mathbf{r}_1)}{l_x} \frac{(l_y - Y)Z}{l_y l_z} \\ &+ \frac{\hat{\omega}(\mathbf{r}_6) - \hat{\omega}(\mathbf{r}_2)}{l_x} \frac{Y(l_z - Z)}{l_y l_z} + \frac{\hat{\omega}(\mathbf{r}_7) - \hat{\omega}(\mathbf{r}_3)}{l_x} \frac{YZ}{l_y l_z}, \end{aligned} \quad (\text{A8})$$

$$\begin{aligned} \frac{\partial \hat{\omega}}{\partial R_{jy}} &= \frac{\hat{\omega}(\mathbf{r}_2) - \hat{\omega}(\mathbf{r}_0)}{l_y} \frac{(l_x - X)(l_z - Z)}{l_x l_z} \\ &+ \frac{\hat{\omega}(\mathbf{r}_6) - \hat{\omega}(\mathbf{r}_4)}{l_y} \frac{X(l_z - Z)}{l_x l_z} \\ &+ \frac{\hat{\omega}(\mathbf{r}_3) - \hat{\omega}(\mathbf{r}_1)}{l_y} \frac{(l_x - X)Z}{l_x l_z} + \frac{\hat{\omega}(\mathbf{r}_7) - \hat{\omega}(\mathbf{r}_5)}{l_y} \frac{XZ}{l_x l_z}, \end{aligned} \quad (\text{A9})$$

and

$$\frac{\partial \hat{\omega}}{\partial R_{jz}} = \frac{\hat{\omega}(\mathbf{r}_1) - \hat{\omega}(\mathbf{r}_0)}{l_z} \frac{(l_x - X)(l_y - Y)}{l_x l_y}$$

$$\begin{aligned} &+ \frac{\hat{\omega}(\mathbf{r}_5) - \hat{\omega}(\mathbf{r}_4)}{l_z} \frac{X(l_y - Y)}{l_x l_y} \\ &+ \frac{\hat{\omega}(\mathbf{r}_3) - \hat{\omega}(\mathbf{r}_2)}{l_z} \frac{(l_x - X)Y}{l_x l_y} + \frac{\hat{\omega}(\mathbf{r}_7) - \hat{\omega}(\mathbf{r}_6)}{l_z} \frac{XY}{l_x l_y}. \end{aligned} \quad (\text{A10})$$

Inserting the above expressions to the BD equation gives the final form which we use in our BD simulations.

We close with two remarks. First, a bead located at $z \leq 0.5$ contributes density only to the 4 nearest mesh points due to the impenetrable boundary condition. This indicates that any bead at $z < 0.5$ acts as if it were at $z = 0.5$. Second, the adsorption potential is usually defined as a steplike function with the potential width the segmental length a ($a \equiv 1$ is the unit length). This means that $U_a(z) = 1$ for $z < 1$ and zero otherwise. In the present case, however, we introduce an assignment function to distribute density to the nearest mesh points, which means that a bead can still feel the force even it is at a location with $z > 1$. Considering the specific form of the assignment function, the apparent potential imposed on a bead should be regulated as $U_a(\mathbf{r}) = \min(1, 3/2 - z)$ for $z < 3/2$, and zero otherwise.

-
- [1] A. Halperin, M. Tirrell, and T. P. Lodge, *Adv. Polym. Sci.* **100**, 31 (1992).
- [2] B. Zhao and W. J. Brittain, *Prog. Polym. Sci.* **25**, 677 (2000).
- [3] K. Kato, E. Uchida, E.-T. Kang, Y. Uyama, and Y. Ikada, *Prog. Polym. Sci.* **28**, 209 (2003).
- [4] O. Azzaroni, *J. Polym. Sci., Part A: Polym. Chem.* **50**, 3225 (2012).
- [5] T. Suo and M. Whitmore, *J. Chem. Phys.* **141**, 204903 (2014).
- [6] S. Qi, L. I. Klushin, A. M. Skvortsov, A. A. Polotsky, and F. Schmid, *Macromolecules* **48**, 3775 (2015).
- [7] S. Zhang, S. Qi, L. I. Klushin, A. M. Skvortsov, D. Yan, and F. Schmid, *J. Chem. Phys.* **147**, 064902 (2017).
- [8] M. Urbakh, J. Klafter, D. Gourdon, and J. Israelachvili, *Nature* **430**, 525 (2004).
- [9] C. Bustamante, J. F. Marko, E. D. Siggia, and S. Smith, *Science* **265**, 1599 (1995).
- [10] S. Smith, Y. Cui, and C. Bustamante, *Science* **271**, 795 (1996).
- [11] M. Rief, J. M. Fernandez, and H. E. Gaub, *Phys. Rev. Lett.* **81**, 4764 (1998).
- [12] A. M. Skvortsov, A. A. Gorbunov, and L. I. Klushin, *J. Chem. Phys.* **100**, 2325 (1994).
- [13] L. I. Klushin, A. M. Skvortsov, and A. A. Gorbunov, *Phys. Rev. E* **56**, 1511 (1997).
- [14] P. G. de Gennes, *Scaling Concepts in Polymer Physics* (Cornell University Press, 1979).
- [15] E. Eisenriegler, *Polymers Near Surfaces* (World Scientific, 1993).
- [16] A. A. Gorbunov and A. M. Skvortsov, *J. Chem. Phys.* **98**, 5961 (1993).
- [17] A. M. Skvortsov, L. I. Klushin, G. J. Fleer, and F. A. M. Leermakers, *J. Chem. Phys.* **132**, 064110 (2010).
- [18] L. I. Klushin and A. M. Skvortsov, *J. Phys. A* **44**, 473001 (2011).
- [19] A. M. Skvortsov, L. I. Klushin, A. A. Polotsky, and K. Binder, *Phys. Rev. E* **85**, 031803 (2012).
- [20] D. Ioffe and Y. Velenik, *Braz. J. Probab. Stat.* **24**, 279 (2010).
- [21] N. R. Beaton, *J. Phys. A: Math. Theor.* **48**, 16FT03 (2015).
- [22] E. J. J. van Rensburg and S. G. Whittington, *J. Phys. A: Math. Theor.* **46**, 435003 (2013).
- [23] E. J. J. van Rensburg and S. G. Whittington, *J. Phys. A: Math. Theor.* **49**, 244001 (2016).
- [24] J. M. Hammersley, G. M. Torrie, and S. G. Whittington, *J. Phys. A: Math. Gen.* **15**, 539 (1982).
- [25] M. Doi and S. F. Edwards, *The theory of polymer dynamics* (Oxford University Press, 1999).
- [26] R. W. Hockney and J. W. Eastwood, *Computer Simulation using Particles* (CRC Press, 1988).
- [27] F. A. Detcheverry, H. Kang, K. C. Daoulas, M. Müller, P. F. Nealey, and J. J. de Pablo, *Macromolecules* **41**, 4989 (2008).
- [28] S. Qi, L. I. Klushin, A. M. Skvortsov, and F. Schmid, *Macromolecules* **49**, 9665 (2016).
- [29] C. K. Birdsall and D. Fuss, *J. Comput. Phys.* **135**, 141 (1997).
- [30] K. Binder and D. W. Heermann, *Monte Carlo Simulation in Statistical Physics: An Introduction* (Springer Berlin Heidelberg, 2010).
- [31] N. Clisby and B. Dünweg, *Phys. Rev. E* **94**, 052102 (2016).
- [32] M. N. Barber, A. J. Guttmann, K. M. Middlemiss, G. M. Torrie, and S. G. Whittington, *J. Phys. A: Math. Gen.* **11**, 1833 (1978).
- [33] M. Lax, *Macromolecules* **7**, 660 (1974).
- [34] P. Mark, S. Windwer, and M. Lax, *Macromolecules* **8**, 946 (1975).

- [35] L. Ma, K. M. Middlemiss, and S. G. Whittington, *Macromolecules* **10**, 1415 (1977).
- [36] A. J. Bray and M. A. Moore, *J. Phys. A: Math. Gen.* **10**, 1927 (1977).
- [37] P. Grassberger, *J. Phys. A: Math. Gen.* **38**, 323 (2005).
- [38] N. Clisby, A. R. Conway, and A. J. Guttmann, *J. Phys. A: Math. Theor.* **49**, 015004 (2016).
- [39] N. Clisby, *J. Phys. A: Math. Theor.* **50**, 264003 (2017).
- [40] M. E. Fisher, *J. Chem. Phys.* **44**, 616 (1966).
- [41] E. A. DiMarzio, *J. Chem. Phys.* **42**, 2101 (1965).
- [42] H.-W. Diehl and M. Shpot, *Nuc. Phys. B* **528**, 595 (1998).
- [43] R. Descas, J.-U. Sommer, and A. Blumen, *J. Chem. Phys.* **120**, 8831 (2004).
- [44] L. I. Klushin, A. A. Polotsky, H.-P. Hsu, D. A. Markelov, K. Binder, and A. M. Skvortsov, *Phys. Rev. E* **87**, 022604 (2013).
- [45] H. Risken, *The Fokker-Planck Equation*, Springer Series in Synergetics, Vol. 18 (Springer, 1996).